QUARTERLY OF APPLIED MATHEMATICS

Vol. VIII APRIL, 1950 No. 1

A CONTRIBUTION TO THE HYDRODYNAMICS OF LUBRICATION*

BY

GREGORY H. WANNIER

*Socony-Vacuum Laboratories, Paulsboro, N. J.***

1. Introduction. It has been known for a long time that the lubrication of solid surfaces by fluids is primarily an effect of their viscosity. Today, however, there is a widespread belief that there are other, as yet unknown, properties of liquids entering into the picture, particularly at high pressures. An investigation of such effects is severely hampered by the fact that there are few experimental results that can be checked against theory. This is due partly to the difficulties of making precise experimental measurements, and partly to the insufficient development of the conventional theory.

This paper applies conventional theory to a few situations of experimental interest. In Sec. 2, a comparison is made between the Reynolds equation and the more accurate Stokes equations. Section 3 studies the cylindrical bearing without assuming film lubrication, while Sec. 4 studies the spherical bearing as a sample of a case with side leakage.

2. The equations of Reynolds and Stokes. A good starting point for the study of lubrication are the Stokes equations of hydrodynamics,[1]

$$\nabla p = \eta \nabla^2 \mathbf{v}, \tag{1}$$

$$\nabla \cdot \mathbf{v} = 0, \tag{2}$$

with their immediate consequence

$$\nabla^2 p = 0. \tag{3}$$

The relations (1) to (3) are already a special case of the general hydrodynamic theory. They assume: (a) that the inertia of the liquid can be neglected; (b) that the liquid is incompressible; and (c) that the viscosity η is a constant independent of applied stresses.

Assumption (a) is probably justified if the equations are used primarily for the study of stresses, for one can easily verify that the pressures obtained from Bernoulli's theorem are of an order of magnitude smaller than the pressures significant in lubrication theory. This still leaves the possibility that the flow pattern in regions of low stress may come out wrong because of this neglect. Assumption (b), on the other hand, is very serious indeed. The Eqs. (1) and (2) always lead to negative pressures that may equal thousands of atmospheres. We know with a high degree of certainty that such pressures cannot

*Received Feb. 24, 1949.

**Now at Bell Telephone Laboratories, Murray Hill, N. J.

[1]Lamb, *Hydrodynamics*, Cambridge University Press, 1932, p. 595.

exist in an actual lubricant.[2] The most plausible way by which the fluid presumably escapes these pressures is cavitation. But a coherent hydrodynamical method which takes account of cavitation is not available at this time. We are limited, therefore, to qualitative guesses concerning such a development. Assumption (c) is also incorrect since it has been shown that viscosity is dependent on pressure and shearing rate. It seems reasonable at this time, however, to expect no qualitative change from a more refined treatment of viscosity.

Almost all the calculations on lubrication found in the literature proceed not from the equations of Stokes given above, but from a two-dimensional equation of Reynolds.[3] Reynolds' treatment is known to be more approximate than the treatment of Stokes and to be applicable mainly to thin lubricating films; but beyond this, their mutual relation is not well understood.

In order to clear up this point we shall consider the following specialized situation. Suppose we have a thin layer of liquid which is bounded on one side by an ideal sta-

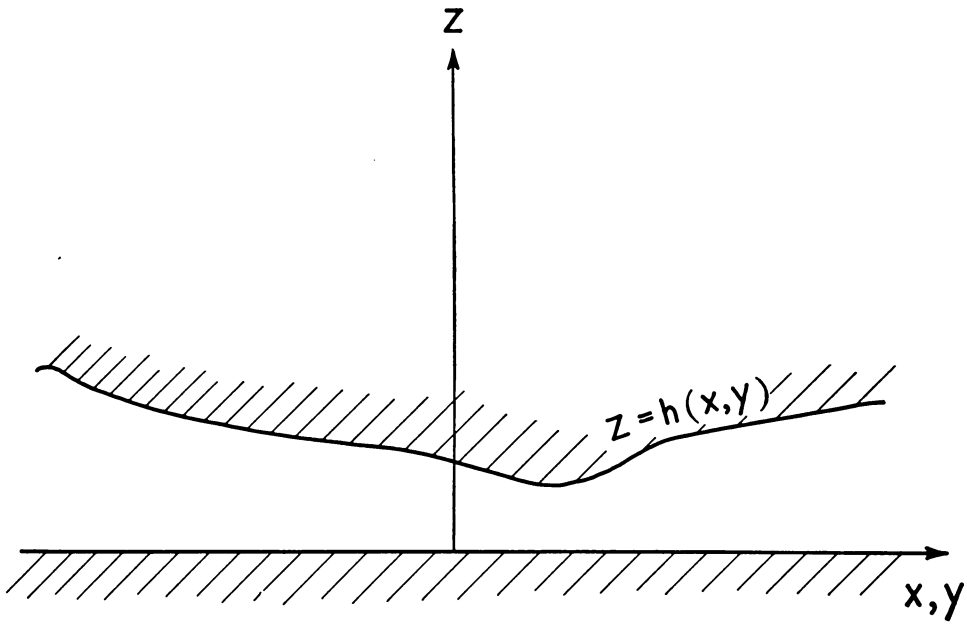

FIG. 1. A sample case for examining the Reynolds equation.

tionary plane, which we take as the xy-plane (Fig. 1), and on the other side by an arbitrary surface

$$z = h(x, y). \tag{4}$$

Let this surface be moving with a velocity whose components are U, V, W which are functions of x and y.

[2]Swift, Proc. Inst. Civ. Eng. **233**, 267 (1932); Scott, Shoemaker, Tanner & Wendel, J. Chem. Phys. **16**, 495 (1948); Briggs, Johnson, & Mason, J. Acoust. Soc. Amer. **19**, 664 (1947); Fisher, J. Appl. Phys. **19**, 1062 (1948).

[3]O. Reynolds, Phil. Trans. Roy. Soc. **177**, 157 (1886).

We now introduce power series developments. For the pressure p we set

$$\frac{1}{\eta} p(x, y, z) = \sum_{\nu=0}^{\infty} \pi_\nu(x, y) z^\nu, \tag{5a}$$

and for the components u, v, w within the liquid

$$u(x, y, z) = \sum_{\nu=0}^{\infty} \xi_\nu(x, y) z^\nu, \tag{5b}$$

$$v(x, y, z) = \sum_{\nu=0}^{\infty} \eta_\nu(x, y) z^\nu, \tag{5c}$$

$$w(x, y, z) = \sum_{\nu=0}^{\infty} \zeta_\nu(x, y) z^\nu. \tag{5d}$$

Equations (1), (2) and (3) then become

$$\frac{\partial \pi_\nu}{\partial x} = \frac{\partial^2 \xi_\nu}{\partial x^2} + \frac{\partial^2 \xi_\nu}{\partial y^2} + (\nu + 2)(\nu + 1)\xi_{\nu+2}, \tag{6a}$$

$$\frac{\partial \pi_\nu}{\partial y} = \frac{\partial^2 \eta_\nu}{\partial x^2} + \frac{\partial^2 \eta_\nu}{\partial y^2} + (\nu + 2)(\nu + 1)\eta_{\nu+2}, \tag{6b}$$

$$(\nu + 1)\pi_{\nu+1} = \frac{\partial^2 \zeta_\nu}{\partial x^2} + \frac{\partial^2 \zeta_\nu}{\partial y^2} + (\nu + 2((\nu + 1)\zeta_{\nu+2}, \tag{6c}$$

$$(\nu + 1)\zeta_{\nu+1} + \frac{\partial \xi_\nu}{\partial x} + \frac{\partial \eta_\nu}{\partial y} = 0, \tag{6d}$$

$$\frac{\partial^2 \pi_\nu}{\partial x^2} + \frac{\partial^2 \pi_\nu}{\partial y^2} + (\nu + 2)(\nu + 1)\pi_{\nu+2} = 0. \tag{6e}$$

The boundary conditions are

$$\xi_0 = \eta_0 = \zeta_0 = 0, \tag{7a}$$

$$\sum_{\nu=1}^{\infty} \xi_\nu(x, y) h^\nu(x, y) = U(x, y), \tag{7b}$$

$$\sum_{\nu=1}^{\infty} \eta_\nu(x, y) h^\nu(x, y) = V(x, y), \tag{7c}$$

$$\sum_{\nu=1}^{\infty} \zeta_\nu(x, y) h^\nu(x, y) = W(x, y). \tag{7d}$$

In reducing the system (6) we observe that the quantities ζ_ν can be eliminated and that Eq. (6c) is redundant, except when $\nu = 0$. This leaves the reduced system

$$\frac{\partial \pi_\nu}{\partial x} = \frac{\partial^2 \xi_\nu}{\partial x^2} + \frac{\partial^2 \xi_\nu}{\partial y^2} + (\nu + 2)(\nu + 1)\xi_{\nu+2}\,, \tag{8a}$$

$$\frac{\partial \pi_\nu}{\partial y} = \frac{\partial^2 \eta_\nu}{\partial x^2} + \frac{\partial^2 \eta_\nu}{\partial y^2} + (\nu + 2)(\nu + 1)\eta_{\nu+2}\,, \tag{8b}$$

$$\frac{\partial^2 \pi_\nu}{\partial x^2} + \frac{\partial^2 \pi_\nu}{\partial y^2} + (\nu + 2)(\nu + 1)\pi_{\nu+2} = 0, \tag{8c}$$

$$\pi_1 = -\frac{\partial \xi_1}{\partial x} - \frac{\partial \eta_1}{\partial y}\,, \tag{9}$$

with the reduced boundary conditions

$$\sum_{\nu=1}^{\infty} \xi_\nu(x, y)h^\nu(x, y) = U(x, y), \tag{10a}$$

$$\sum_{\nu=1}^{\infty} \eta_\nu(x, y)h^\nu(x, y) = V(x, y), \tag{10b}$$

$$\sum_{\nu=2}^{\infty} \frac{1}{\nu}\left\{\frac{\partial \xi_{\nu-1}}{\partial x} + \frac{\partial \eta_{\nu-1}}{\partial y}\right\}h^\nu(x, y) = -W(x, y). \tag{10c}$$

We can look at these equations in the following way: the Eqs. (8) determine all the ξ, η and π of index larger than one in terms of π_0, π_1, ξ_1, η_1. These four quantities are determined by the remaining four equations. An actual procedure of this type is generally difficult because (10) involves not only these four variables, but all higher index variables as well.

This is the point where the thin film assumption enters. The Eqs. (8) give us inequalities of the type

$$\pi_{\nu+2}z^{\nu+2} \sim \pi_{\nu+2}h^{\nu+2} \sim \pi_\nu \frac{h^2}{l^2} h^\nu \ll \pi_\nu h^\nu \sim \pi_\nu z^\nu$$

provided

$$\frac{h}{l} \ll 1.$$

Here h is the thickness and l the length of the liquid film. This means that in each parity, higher powers in the series (5) are small compared with lower powers, and we can get a first approximation to a solution by retaining the first term of each parity in (10). This leads to the simplified boundary conditions

$$\xi_1 h + \xi_2 h^2 = U, \tag{11a}$$

$$\eta_1 h + \eta_2 h^2 = V, \tag{11b}$$

$$\frac{1}{2}\left\{\frac{\partial \xi_1}{\partial x} + \frac{\partial \eta_1}{\partial y}\right\}h^2 + \frac{1}{3}\left\{\frac{\partial \xi_2}{\partial x} + \frac{\partial \eta_2}{\partial y}\right\}h^3 = -W. \tag{11c}$$

They have to be combined with the first of the Eqs. (8a) and (8b):

$$\frac{\partial \pi_0}{\partial x} = 2\xi_2 , \tag{11d}$$

$$\frac{\partial \pi_0}{\partial y} = 2\eta_2 . \tag{11e}$$

We thus have the five equations (11) in the five unknowns ξ_1, ξ_2, η_1, η_2, π_0. If we eliminate the first four unknowns from the set, we get

$$\frac{1}{6}\left\{\frac{\partial}{\partial x}\left(h^3 \frac{\partial \pi_0}{\partial x}\right) + \frac{\partial}{\partial y}\left(h^3 \frac{\partial \pi_0}{\partial y}\right)\right\} = 2W - U\frac{\partial h}{\partial x} - V\frac{\partial h}{\partial y} + h\left(\frac{\partial U}{\partial x} + \frac{\partial V}{\partial y}\right).$$

The left-hand side is already Reynolds' equation. For the right-hand side we can distinguish essentially two cases.

(a) We may have a stationary curved surface rotating against our fixed plane (Fig. 2).

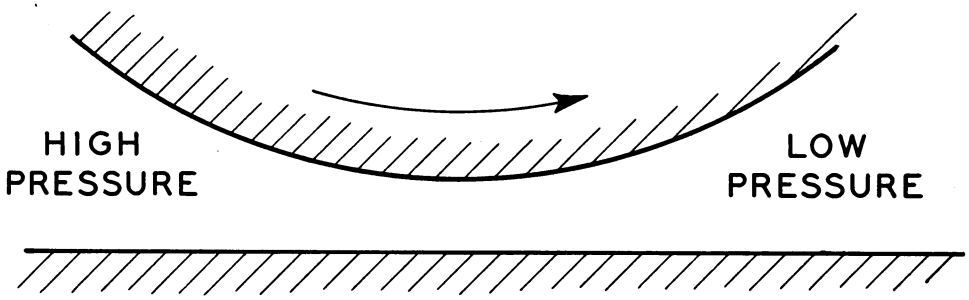

FIG. 2. Situation for the normal Reynolds equation.

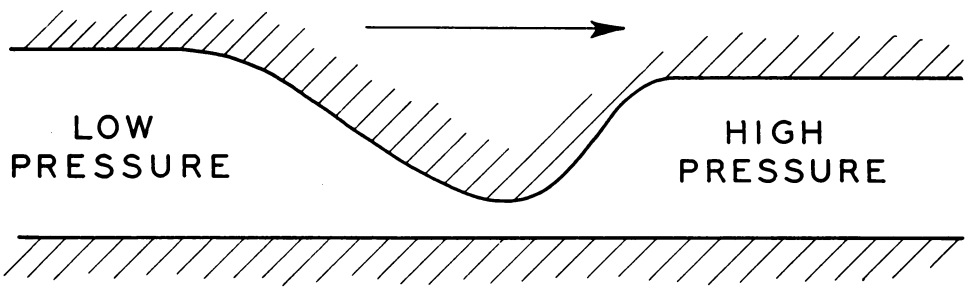

FIG. 3. Situation for the reversed Reynolds equation.

(b) We may have a bump in the moving surface moving parallel to the plane (Fig. 3). In the first case we have that

$$W = U\frac{\partial h}{\partial x} + V\frac{\partial h}{\partial y},$$

and the last two terms are smaller by a factor h/a, where a is the radius of rotation.

In the second case W and the last two terms vanish. Thus we observe that we get the Reynolds equation either way, but in the second case the sign, and hence the location of the pressure maximum and minimum, are reversed, as compared with the usual case. In an actual arrangement h is likely to vary for either reason. We can then make the definitions:

$$h_g = \text{a geometric } h \text{ defined for an ideally smooth surface;} \tag{12a}$$

$$h_r = \text{the remainder of } h \text{ due to roughness.} \tag{12b}$$

We can distinguish h_g and h_r by the fact that the velocity of the moving wall is by definition parallel to its geometric surface, so that h_g is stationary, h_r is variable.

From these considerations, we deduce the final equation:

$$\frac{1}{6}\left\{\frac{\partial}{\partial x}\left(h^3\frac{\partial \pi_0}{\partial x}\right) + \frac{\partial}{\partial y}\left(h^3\frac{\partial \pi_0}{\partial y}\right)\right\} = U\frac{\partial(h_g - h_r)}{\partial x} + V\frac{\partial(h_g - h_r)}{\partial y}. \tag{13}$$

This is Reynolds' equation if $h_r = 0$. In addition to deriving this equation we have obtained a complete description of the flow and pressure pattern through (11) and (9) and the recurrence relations (8) for higher terms. This refinement can be applied, for instance, to the Sommerfeld solution for the cylindrical bearing or to the results of this paper on the spherical bearing.[4] The result is that the approximation proceeds in powers of h/a, where h is the clearance and a the radius, and that there are always pairs of contributions, such as ξ_1 and ξ_2, which are of equal order.

It is clear that the restrictive assumptions made in deriving (13) are unsatisfactory. If one investigates curved oil films, one gets the obvious generalizations of (11) and (13):

$$\mathbf{V} = \mathbf{U}_1 h + \mathbf{U}_2 h^2, \tag{14a}$$

$$\frac{1}{\eta}\nabla\pi_0 = 2\mathbf{U}_2, \tag{14b}$$

$$\frac{1}{6}\nabla\cdot(h^3\nabla\pi_0) = \mathbf{V}\cdot\nabla(h_g - h_r), \tag{15}$$

where all vector quantities are understood to be tangential to the liquid film. The attempt to remove the restriction illustrated in Fig. 1, however, was not successful. But it stands to reason that (14) and (15) should be derivable even if both surfaces have irregular shape and proper velocities. The work of later sections and general plausibility arguments indicate that the proper generalization of (15) is

$$\frac{1}{6}\nabla\cdot(h^3\nabla\pi_0) = (\mathbf{V}_1 + \mathbf{V}_2)\cdot\left\{\nabla h_g - \left|\frac{\mathbf{V}_1 - \mathbf{V}_2}{\mathbf{V}_1 + \mathbf{V}_2}\right|\nabla h_r\right\}. \tag{16}$$

We have thus been able to show, at least for a special situation, that the Reynolds equation arises from the Stokes equations in first approximation if all quantities entering the Stokes equations are expanded in powers of the film thickness. In addition, we have obtained simple formulas which give such unknowns as the transverse pressure gradient from the Reynolds solution.[4] The standard assumption that the latter is zero is, therefore, superfluous.

[4]See Eqs. (40) and (59).

3. The cylindrical bearing. It has been pointed out by Duffing and by Reissner[5] that the equations of Stokes can be solved rigorously for the infinite cylindrical bearing. The derivation to follow will proceed to the end, giving explicit expressions for the resultant forces and torques. Several limiting cases will be presented, one of which is the classical Sommerfeld solution.[6]

The infinite cylindrical bearing has flow in two dimensions only (no side leakage). The Stokes equations (1) and (2) reduce, for such a case, to

$$\frac{\partial p}{\partial x} = \eta\left(\frac{\partial^2 u}{\partial x^2} + \frac{\partial^2 u}{\partial y^2}\right), \tag{17a}$$

$$\frac{\partial p}{\partial y} = \eta\left(\frac{\partial^2 v}{\partial x^2} + \frac{\partial^2 v}{\partial y^2}\right), \tag{17b}$$

$$\frac{\partial u}{\partial x} + \frac{\partial v}{\partial y} = 0, \tag{18}$$

for the interspace between two circles of radius a_1 and a_2. The circles are placed eccentrically by an amount e (Fig. 4). At each boundary the normal velocity must vanish and the tangential velocity must equal a specified constant amount v_1 and v_2, respectively.

The equations are solved most conveniently by first solving (18) identically through the introduction of a stream function Ψ:

$$u = -\frac{\partial \Psi}{\partial y}, \tag{19a}$$

$$v = \frac{\partial \Psi}{\partial x}. \tag{19b}$$

Then if we substitute (19) into (17), we find that we have to solve the equation

$$\nabla^2\nabla^2\Psi = 0 \tag{20}$$

and that p will be obtained from $\nabla^2\Psi$ by the method of conjugate functions:

$$\nabla^2\Psi + i\frac{1}{\eta}p = f(x + iy). \tag{21}$$

The conditions under which Eq. (20) must be solved are that: (a) Ψ must be a constant on each of the two bounding circles; (b) the normal gradient of Ψ on each specified circle must equal a specified constant, v_1 or v_2; (c) the conjugate function of $\nabla^2\Psi$ must be single-valued over the entire domain.

Conditions (a) and (b) are somewhat weaker than the standard boundary conditions for (20).[7] Condition (c) which replaced the missing boundary conditions might be expected to be awkward. Actually, it gives no trouble in the following applications.

---

[5]G. Duffing, Z. angew Math. Mech. **4**, 296 (1924); H. Reissner, Z. angew Math. Mech. **15**, 81 (1935).

[6]A. Sommerfeld, Z. Math. Phys. **50**, 97 (1904).

[7]See Frank-v. Mises., *Differentialgleichungen der Physik*, vol. I, pp. 845-862.

The solution of (20) may be constructed with the help of a general theorem[7] which states that any solution of (20) can be written in either of the following two forms:

$$\Psi = y\Phi_1 + \Phi_2 , \tag{22a}$$

or

$$\Psi = (x^2 + y^2)\Phi_1 + \Phi_2 , \tag{22b}$$

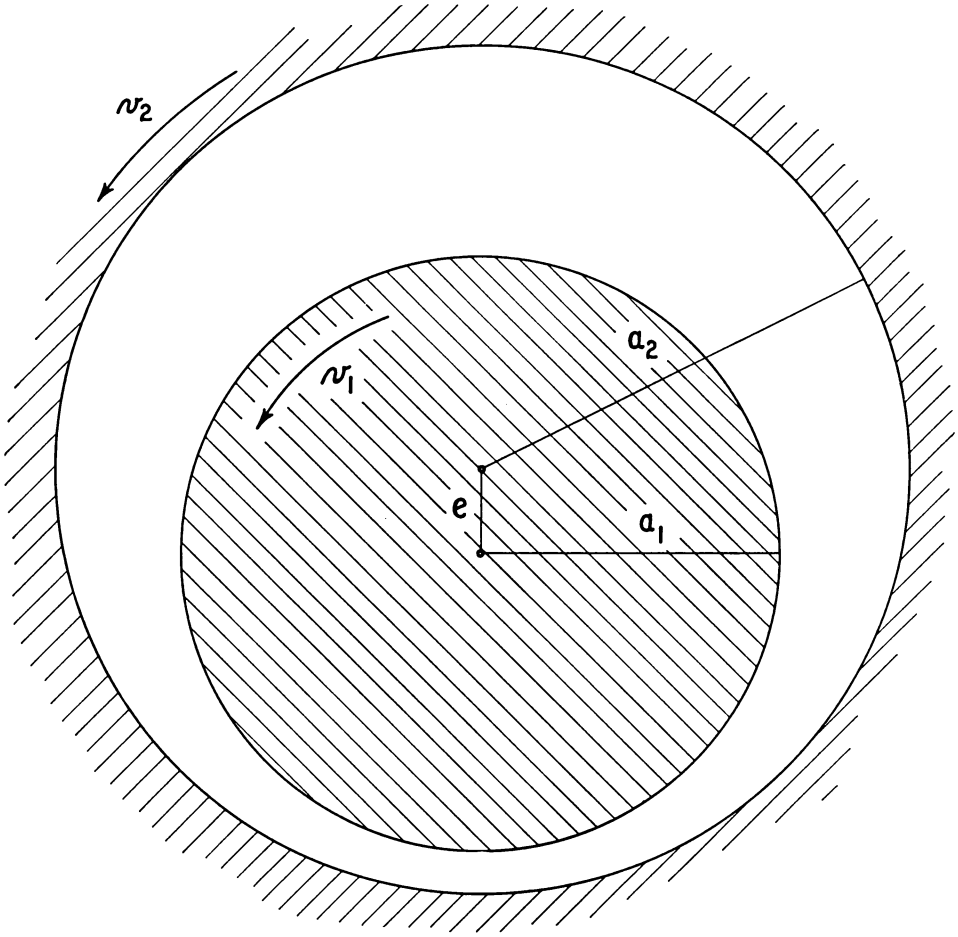

FIG. 4. Basic data for the cylindrical bearing.

where

$$\nabla^2\Phi_1 = \nabla^2\Phi_2 = 0 \tag{22c}$$

and x and y are Cartesian coordinates. This theorem associates (20) very closely with the Laplace equation

$$\nabla^2\Phi = 0.$$

The electrostatic solution for the geometry of Fig. 4 is well-known. In order to express

it simply we pick a coordinate system as shown in Fig. 5. The y-axis is laid through the centers C_1 and C_2 of the two circles to an external origin O. The distances OC_1 and OC_2 will be denoted, respectively, by d_1 and d_2. The origin is located in such a way that

$$d_1^2 - a_1^2 = d_2^2 - a_2^2 = s^2. \tag{23}$$

Equation (23) and the definition

$$d_2 - d_1 = e \tag{24}$$

give us d_1, d_2, s in terms of the original quantities a_1, a_2, e of Fig. 4. We find that

$$d_1 = \frac{1}{2e}(a_2^2 - a_1^2) - \frac{1}{2}e, \tag{25a}$$

$$d_2 = \frac{1}{2e}(a_2^2 - a_1^2) + \frac{1}{2}e, \tag{25b}$$

$$s^2 = \frac{1}{4e^2}(a_2 - a_1 - e)(a_2 - a_1 + e)(a_2 + a_1 + e)(a_2 + a_1 - e). \tag{26}$$

The points A and B on the y-axis, whose distance from 0 is s, serve as origins for the logarithmic potential which is adapted to the present geometry:

$$\Phi = C \log \frac{\overline{BP}}{\overline{AP}} \cdot \tag{27a}$$

The curves on which Φ is constant are circles, two of which are the bounding circles discussed above. If we introduce the variable parameter α for the radius of such a circle and δ for the distance of its center from the origin, we then get the generalization of (23),

$$\delta^2 - \alpha^2 = s^2, \tag{28}$$

and

$$\Phi = \frac{1}{2} C \log \frac{\delta + s}{\delta - s} \cdot \tag{27b}$$

This solution Φ and its derivatives can be used in conjunction with the theorem (22) to produce a large number of solutions of (20). The successful combination is found to have the form

$$\begin{aligned}\Psi = A \log \frac{x^2 + (s+y)^2}{x^2 + (s-y)^2} + B \frac{y(s+y)}{x^2 + (s+y)^2} + C \frac{y(s-y)}{x^2 + (s-y)^2} \\ + Dy + E(x^2 + y^2 + s^2) + Fy \log \frac{x^2 + (s+y)^2}{x^2 + (s-y)^2},\end{aligned} \tag{29a}$$

or, more briefly, in a (δ, y) coordinate system,

$$\begin{aligned}\Psi = A \log \frac{\delta + s}{\delta - s} + B \frac{s + y}{2(\delta + s)} + C \frac{s - y}{2(\delta - s)} + Dy \\ + E \cdot 2\delta y + Fy \log \frac{\delta + s}{\delta - s} \cdot\end{aligned} \tag{29b}$$

Here A, B, C, D, E, F are constants to be determined. The structure of the solution is clear from (29b); we have picked all solutions of (20) which are linear in y on either limit circle. One solution of this form was not admitted, however, namely

$$(x^2 + y^2 + s^2) \log \frac{x^2 + (s + y)^2}{x^2 + (s - y)^2} = 2y\delta \log \frac{\delta + s}{\delta - s} \cdot$$

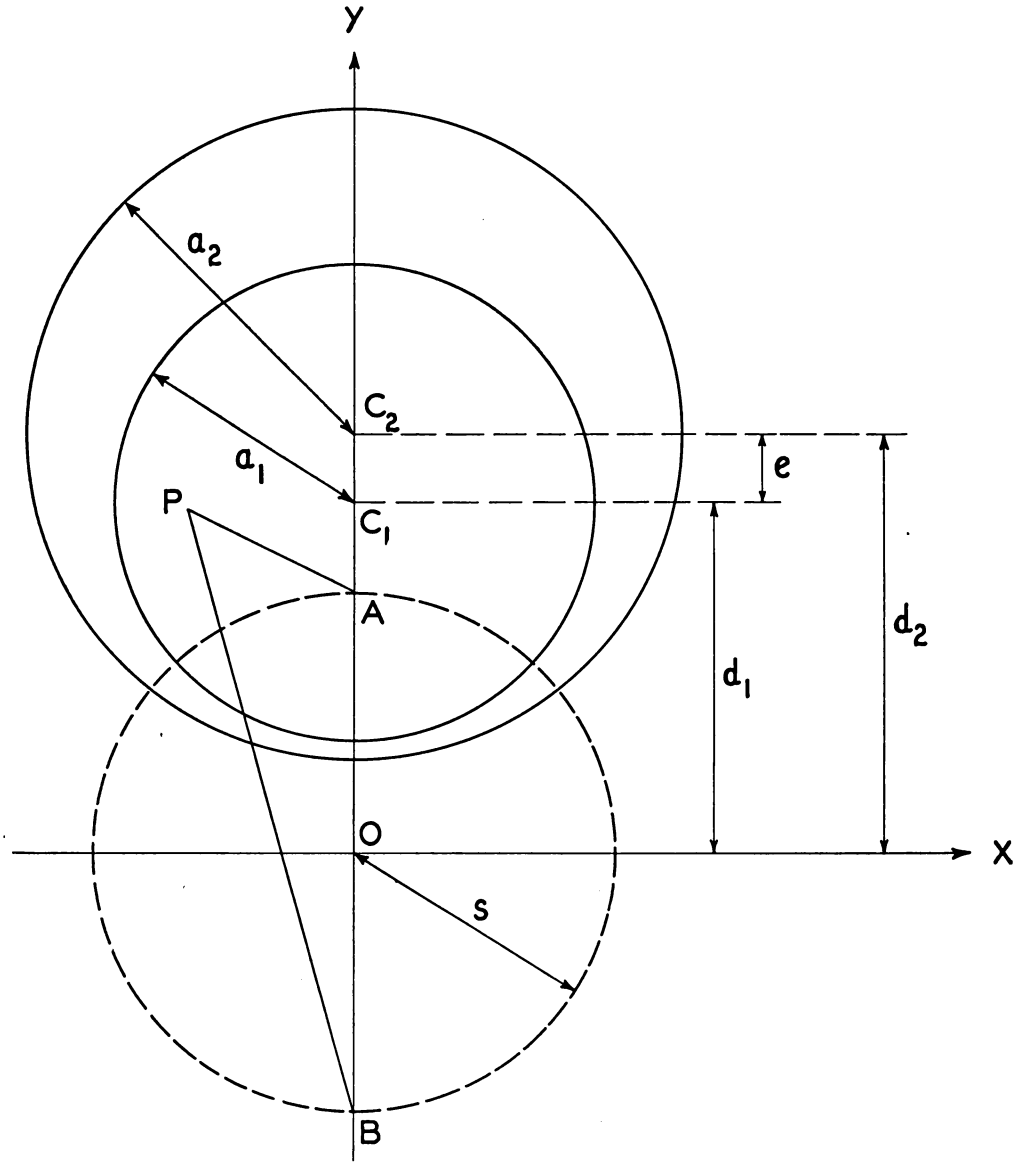

FIG. 5. Geometric parameters for the eccentric bearing.

One verifies easily that a term of this type gives rise to a pressure term which is not single-valued. It must, therefore, be rejected according to condition (c).

The six constants A, B, C, D, E, F are determined by the boundary conditions (a) and (b). Since Ψ is linear in y on either limit circle, we get from (a) two conditions, annulling the linear part on either circle. Now $\partial\Psi/\partial n$ is found to be linear in $1/y$; this gives rise to four more conditions, two of them setting the coefficient of $1/y$ equal to zero and two prescribing the value of the constant. Thus we end up with the following six equations:

$$\frac{1}{2}\frac{1}{d_1+s}B - \frac{1}{2}\frac{1}{d_1-s}C + D + 2d_1E + \log\frac{d_1+s}{d_1-s}F = 0, \tag{30a}$$

$$\frac{1}{2}\frac{1}{d_2+s}B - \frac{1}{2}\frac{1}{d_2-s}C + D + 2d_2E + \log\frac{d_2+s}{d_2-s}F = 0, \tag{30b}$$

$$2A + \frac{1}{2}\frac{d_1-s}{d_1+s}B + \frac{1}{2}\frac{d_1+s}{d_1-s}C = 0, \tag{30c}$$

$$2A + \frac{1}{2}\frac{d_2-s}{d_2-s}B + \frac{1}{2}\frac{d_2+s}{d_2-s}C = 0, \tag{30d}$$

$$\frac{1}{2}\frac{d_1-s}{d_1+s}B - \frac{1}{2}\frac{d_1+s}{d_1-s}C - 2a_1^2E + 2sF = -a_1v_1\,, \tag{30e}$$

$$\frac{1}{2}\frac{d_2-s}{d_2+s}B - \frac{1}{2}\frac{d_2+s}{d_2-s}C - 2a_2^2E + 2sF = -a_2v_2\,. \tag{30f}$$

These equations yield:

$$A = -\frac{1}{2}(d_1d_2 - s^2) \cdot \left\{\frac{2(d_2^2-d_1^2)(a_1v_1+a_2v_2)}{(a_2^2+a_1^2)[(a_2^2+a_1^2)\log\{(d_1+s)(d_2-s)/(d_1-s)(d_2+s)\} - 4se]} + \frac{a_1^2a_2^2(a_1^{-1}v_1 - a_2^{-1}v_2)}{s(a_1^2+a_2^2)(d_2-d_1)}\right\}, \tag{31a}$$

$$B = (d_1+s)(d_2+s)\{\text{same curly bracket}\}, \tag{31b}$$

$$C = (d_1-s)(d_2-s)\{\text{same curly bracket}\}, \tag{31c}$$

$$D = \frac{d_1\log\{(d_2+s)/(d_2-s)\} - d_2\log\{(d_1+s)/(d_1-s)\}}{(a_1^2+a_2^2)\log\{(d_1+s)(d_2-s)/(d_1-s)(d_2+s)\} - 4se}(a_1v_1+a_2v_2) - \frac{2s[(a_2^2-a_1^2)/(a_2^2+a_1^2)](a_1v_1+a_2v_2)}{(a_1^2+a_2^2)\log\{(d_1+s)(d_2-s)/(d_1-s)(d_2+s)\} - 4se} - \frac{a_1^2a_2^2(a_1^{-1}v_1 - a_2^{-1}v_2)}{(a_1^2+a_2^2)e}, \tag{31d}$$

$$E = \frac{(1/2)\log\{(d_1+s)(d_2-s)/(d_1-s)(d_2+s)\}(a_1v_1+a_2v_2)}{(a_1^2+a_2^2)\log\{(d_1+s)(d_2-s)/(d_1-s)(d_2+s)\}-4se}, \tag{31e}$$

$$F = \frac{e(a_1v_1+a_2v_2)}{(a_1^2+a_2^2)\log\{(d_1+s)(d_2-s)/(d_1-s)(d_2+s)\}-4se}. \tag{31f}$$

From the flow pattern, which is completely specified by (29) and (31), we can determine the pressure by using (21). We find that

$$\frac{1}{\eta}p = -B\frac{x(s+y)}{y^2(\delta+s)^2} - C\frac{x(s-y)}{y^2(\delta-s)^2} - F\frac{4sx}{y(\delta^2-s^2)}. \tag{32}$$

Calculation of the forces requires, of course, the entire stress tensor. In our case, the tensor has three components which are obtained as follows:

$$\pi_{xx} = -p - 2\eta\frac{\partial^2\Psi}{\partial x\,\partial y},$$

$$\pi_{yy} = -p + 2\eta\frac{\partial^2\Psi}{\partial x\,\partial y},$$

$$\pi_{xy} = \eta\left(\frac{\partial^2\Psi}{\partial x^2} - \frac{\partial^2\Psi}{\partial y^2}\right).$$

The result is:

$$\begin{aligned}\frac{1}{\eta}\pi_{xx} = {} & -4A\frac{sx(2\delta y-\delta^2-s^2)}{y^2(\delta^2-s^2)^2} - B\frac{x[2y^2+(s-3\delta)y-2s\delta]}{y^2(\delta+s)^3} \\ & + C\frac{x[2y^2-(s+3\delta)y+2s\delta]}{y^2(\delta-s)^3} - 4F\frac{sx(2\delta y-3\delta^2+s^2)}{y^2(\delta^2-s^2)^2},\end{aligned} \tag{33a}$$

$$\begin{aligned}\frac{1}{\eta}\pi_{yy} = {} & 4A\frac{sx(2\delta y-\delta^2-s^2)}{y^2(\delta^2-s^2)^2} + B\frac{x[2y^2+(3s-\delta)y+2s^2]}{y^2(\delta+s)^3} \\ & - C\frac{x[2y^2-(3s+\delta)y+2s^2]}{y^2(\delta-s)^3} + 4F\frac{sx(2\delta y-\delta^2-s^2)}{y(\delta^2-s^2)^2},\end{aligned} \tag{33b}$$

$$\begin{aligned}\frac{1}{\eta}\pi_{xy} = {} & 4A\frac{s[-2\delta y^2+(3\delta^2+s^2)y-2\delta s^2]}{y^2(\delta^2-s^2)^2} \\ & + B\frac{-2y^3+2(2\delta-s)y^2+(3\delta s-2s^2-\delta^2)y+s^2(\delta-s)}{y^2(\delta+s)^3} \\ & - C\frac{-2y^3+2(2\delta+s)y^2-(3\delta s+2s^2+\delta^2)y+s^2(\delta+s)}{y^2(\delta-s)^3} \\ & + 4F\frac{s[-2\delta y^2+4\delta^2y-\delta(\delta^2+s^2)]}{y(\delta^2-s^2)^2}.\end{aligned} \tag{33c}$$

The main interest centers usually on those resultants of (33) which act on the pin or bearing, when considered as rigid bodies. The equations for the components of force acting upon a circle of parameter δ are:

$$\pm F_x = L \oint \left(\pi_{xx} \frac{x}{\alpha} + \pi_{xy} \frac{y - \delta}{\alpha}\right) dl_\delta ,$$

$$\pm F_y = L \oint \left(\pi_{xy} \frac{x}{\alpha} + \pi_{yy} \frac{y - \delta}{\alpha}\right) dl_\delta .$$

We find for these expressions:

$$\pm F_x = 8\pi\eta LF = W, \tag{34a}$$

where F is given by (31f) and L is the length of the cylindrical bearing. Similarly,

$$F_y = 0. \tag{34b}$$

This equation is due to the anti-symmetry of the pressure pattern about the line of centers (cf. Fig. 10). This same symmetry precludes the transport of x momentum into any of the circles, and thus makes the force independent of the parameter δ. The sign depends, of course, on the side from which the force is acting.

Substituting (31f) into (34) we get explicitly that

$$W = \frac{8\pi\eta Le(a_1v_1 + a_2v_2)}{(a_1^2 + a_2^2) \log \{(d_1 + s)(d_2 - s)/(d_1 - s)(d_2 + s)\} - 4se} . \tag{35}$$

The geometrical parameters entering into this equation are explained in Fig. 4, Fig. 5 and Eqs. (23) to (26).

The total torque depends on the choice of the fulcrum. Taking the fulcrum at the center of the circle of parameter δ, we find that

$$\pm T = L\alpha \oint \left\{(\pi_{xx} - \pi_{yy}) \frac{x(\delta - y)}{\alpha^2} + \pi_{xy} \frac{x^2 - (\delta - y)^2}{\alpha^2}\right\} dl_\delta ,$$

or that

$$\pm T = 8\pi\eta L(A + F\delta), \tag{36a}$$

where A and F are constants given by (31a) and (31f). This reduces for the inner surface to

$$T_1 = 8\pi\eta L(A + Fd_1) \tag{36b}$$

and for the outer surface to

$$T_2 = -8\pi\eta L(A + Fd_2). \tag{36c}$$

If torques are referred to the same fulcrum throughout, such as the origin, then a constant torque

$$\pm T = 8\pi\eta LA$$

results. This constancy can again be checked from symmetry considerations.

A convenient way of representing the resultant torque is by calculating the coefficient of friction f. The generally used definition is

$$f_i = \frac{|T_i|}{a_i W}, \tag{37}$$

where T_i is the torque referred to the center of either circle and a_i is its radius. It should be emphasized here that we get two coefficients of friction, one for the inner cylinder and one for the outer cylinder. If we assume the outer surface stationary, we find for the inner surface that

$$f_1 = \frac{a_2^2(d_1d_2 - s^2)[(a_1^2 + a_2^2) \log \{(d_1 + s)(d_2 - s)/(d_1 - s)(d_2 + s)\} - 4se]}{2a_1se^2(a_1^2 + a_2^2)} + \frac{a_1e}{a_1^2 + a_2^2} \tag{38a}$$

and for the outer surface that

$$f_2 = \frac{a_2(d_1d_2 - s^2)[(a_1^2 + a_2^2) \log \{(d_1 + s)(d_2 - s)/(d_1 - s)(d_2 + s)\} - 4se]}{2se^2(a_1^2 + a_2^2)} - \frac{a_2e}{a_1^2 + a_2^2}. \tag{38b}$$

The f generally calculated in the literature is f_1, although many experimental arrangements actually measure the torque on the outer surface.

A good deal of insight into the nature of the solution can be gained by considering limiting cases. We are starting off with the most important one.

(a) *The Sommerfeld-Reynolds limit*: $e = d_2 - d_1 \to 0$.

We expand our results in powers of e and retain only the first term. Let us define the nominal clearance c as

$$a_2 - a_1 = c \tag{39}$$

and write further that

$$a_1 \sim a_2 \sim a.$$

From (25)

$$d_1 \sim d_2 \sim \frac{ac}{e}$$

and from (26)

$$s = \frac{a}{e}(c^2 - e^2)^{1/2}.$$

Then we find for the pressure from (32),

$$p = -\frac{6\eta e(a_1v_1 + a_2v_2)(2c - e \cos \psi) \sin \psi}{(2c^2 + e^2)(c - e \cos \psi)^2}, \tag{40}$$

where ψ is the azimuth measured along the oil film in a counter-clockwise direction, starting from the point of minimum clearance.

Equation (40) is obtainable directly from the Reynolds equation (11) and has been so obtained by Sommerfeld.[6]

The same limiting process can be carried out on the resultant force and torque. For the total force we get

$$W = \frac{12\pi\eta Lea^2(v_1 + v_2)}{(2c^2 + e^2)(c^2 - e^2)^{1/2}} \tag{41}$$

with the usual ambiguity in the sign. For the torques we find that

$$T_1 = \frac{4\pi\eta La^2\{v_2(c^2 - e^2) - v_1(c^2 + 2e^2)\}}{(2c^2 + e^2)(c^2 - e^2)^{1/2}}, \tag{42a}$$

$$T_2 = \frac{4\pi\eta La^2\{v_1(c^2 - e^2) - v_2(c^2 + 2e^2)\}}{(2c^2 + e^2)(c^2 - e^2)^{1/2}}. \tag{42b}$$

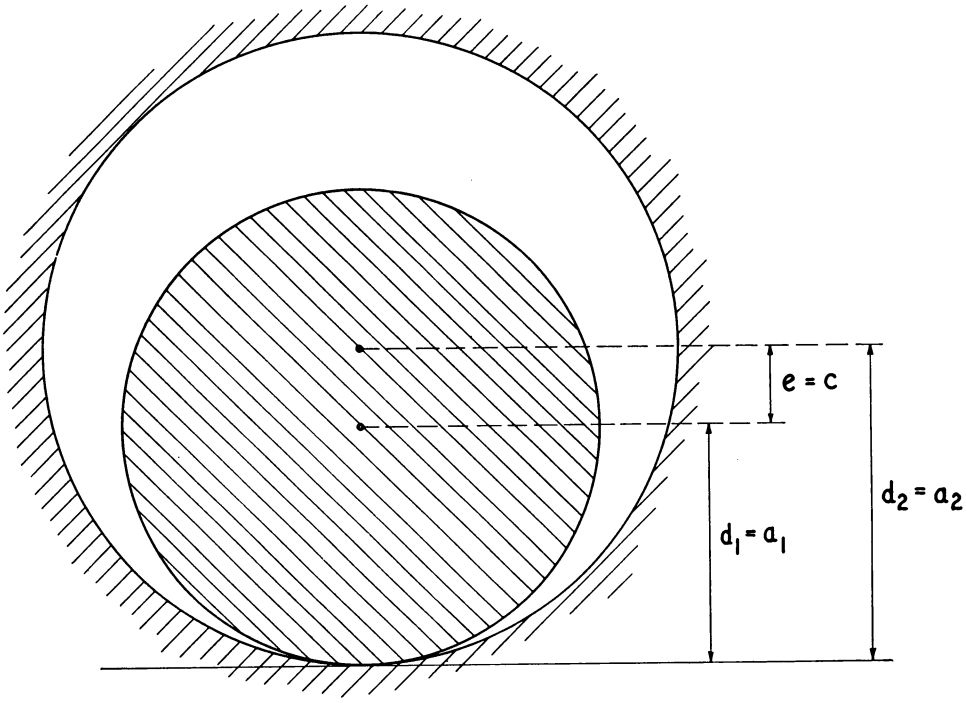

FIG. 6. Limit of zero clearance.

The coefficients of friction reduce to

$$f_1 = \frac{1}{3}\frac{c^2 + 2e^2}{ea}, \tag{43a}$$

$$f_2 = \frac{1}{3}\frac{c^2 - e^2}{ea}. \tag{43b}$$

The formulas for W, T_1 and f_1 can be found in standard textbooks. The flow pattern reduces in this limit to a superposition of viscous drag by the inner cylinder plus a Poiseuille type flow from the high to the low pressure region. This latter flow is opposed to the motion of the pin on the side of wide clearance.

(*b*) *Limit of zero clearance*: $s \to 0$.

This limit, shown in Fig. 6, has some interest. From the experimental side, we observe

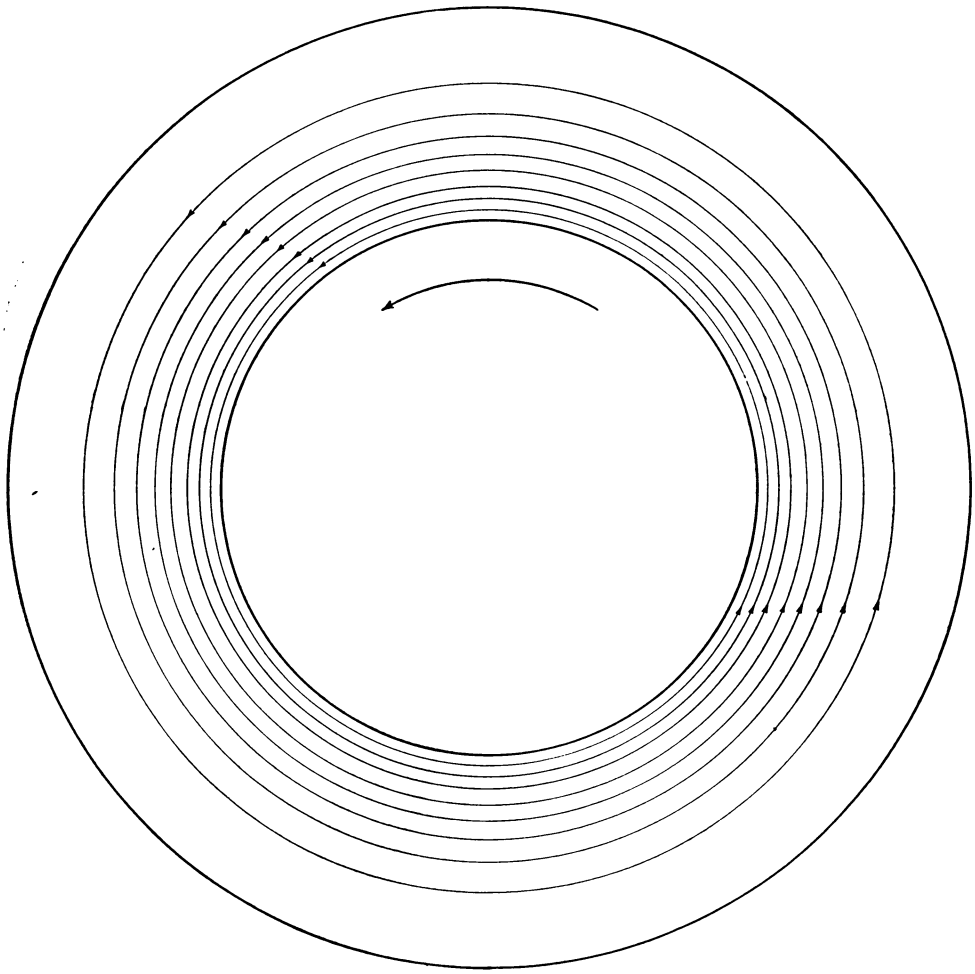

FIG. 7. Streamlines for a journal bearing of diameter ratio 5:9. Case of no eccentricity.

that a loaded bearing usually comes very close to a situation where there is contact along a line or in a point. Mathematically, the simplification obtained is considerable, mainly because the basic solution (27) is now rational instead of logarithmic. In addition, the distinction between d_i and a_i, δ and α, or c and e disappears. As a consequence, the entire system of equations (29) and (31) is now replaced by the short expression

$$\Psi = \frac{y}{\alpha^2 c^2} \{a_1 v_1(\alpha - a_2) + a_2 v_2(\alpha - a_1)\}(\alpha - a_1)(\alpha - a_2) \tag{44}$$

and (32) is replaced by

$$p = -\frac{2\eta a_1^2 a_2^2}{c}\frac{x}{\alpha^2 y}\left\{(v_1 + v_2)\left(\frac{1}{y} - \frac{2}{\alpha} + \frac{2}{a_2} + \frac{2}{a_1}\right) - \frac{v_1}{a_1} - \frac{v_2}{a_2}\right\}. \tag{45}$$

This case is very favorable for a study of flow conditions. The infinities in the stresses, on the other hand, give rise to an infinite force and infinite inner torque. The coefficient of friction stays finite, however, and is

$$f_1 = \frac{a_2 - a_1}{a_1} = \frac{c}{a_1}\,. \tag{46}$$

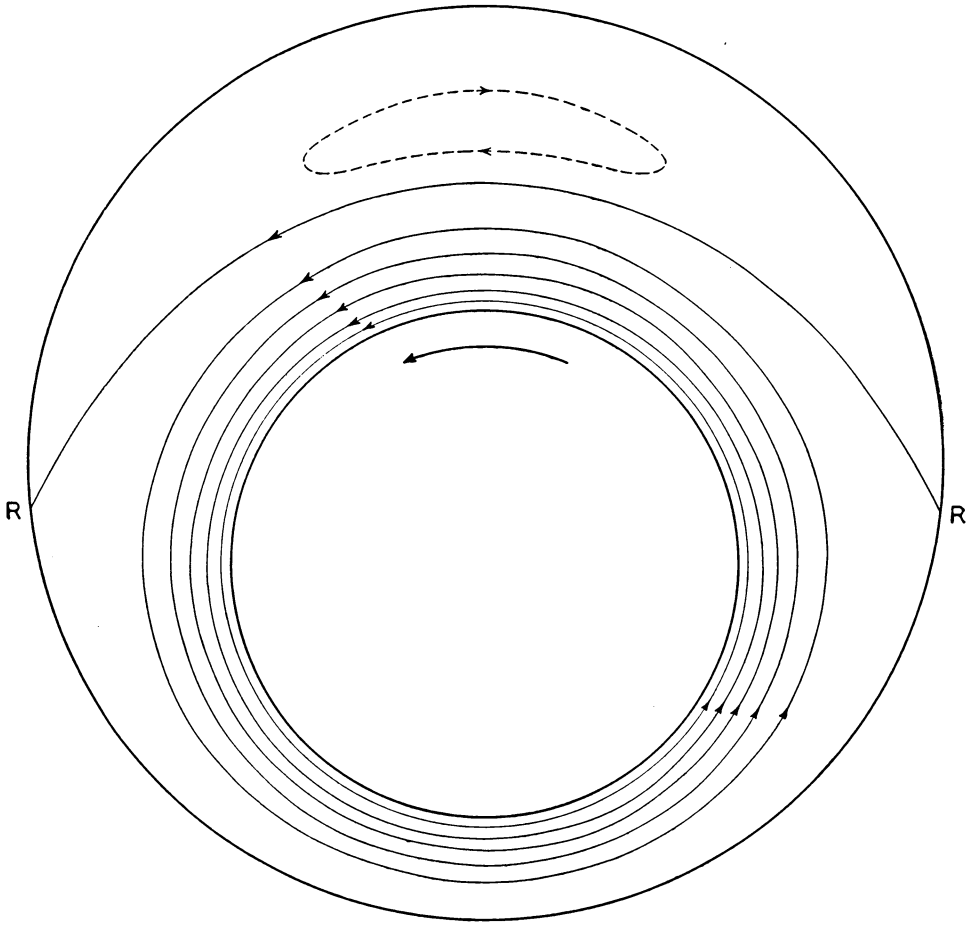

FIG. 8. Streamlines for a journal bearing of diameter ratio 5:9. 50% eccentricity. R = points of flow reversal on stationary surface.

Another finite result for this limiting process is

$$T_2 = 0. \tag{47}$$

Neither (46) nor (47) has much practical significance, since each is obtained by a cancellation of infinities.

(*c*) *Limit of concentric cylinders*: $d_1 \sim d_2 \to \infty$; $d_2 - d_1 \to 0$; a_1, a_2 finite. This complicated passage to the limit gives well-known results. We find that

$$\Psi = \frac{1}{2}\frac{a_2 v_2 - a_1 v_1}{a_2^2 - a_1^2} r^2 + \frac{a_1^2 a_2^2 (a_1^{-1} v_1 + a_2^{-1} v_2)}{a_2^2 - a_1^2} \log r, \tag{48}$$

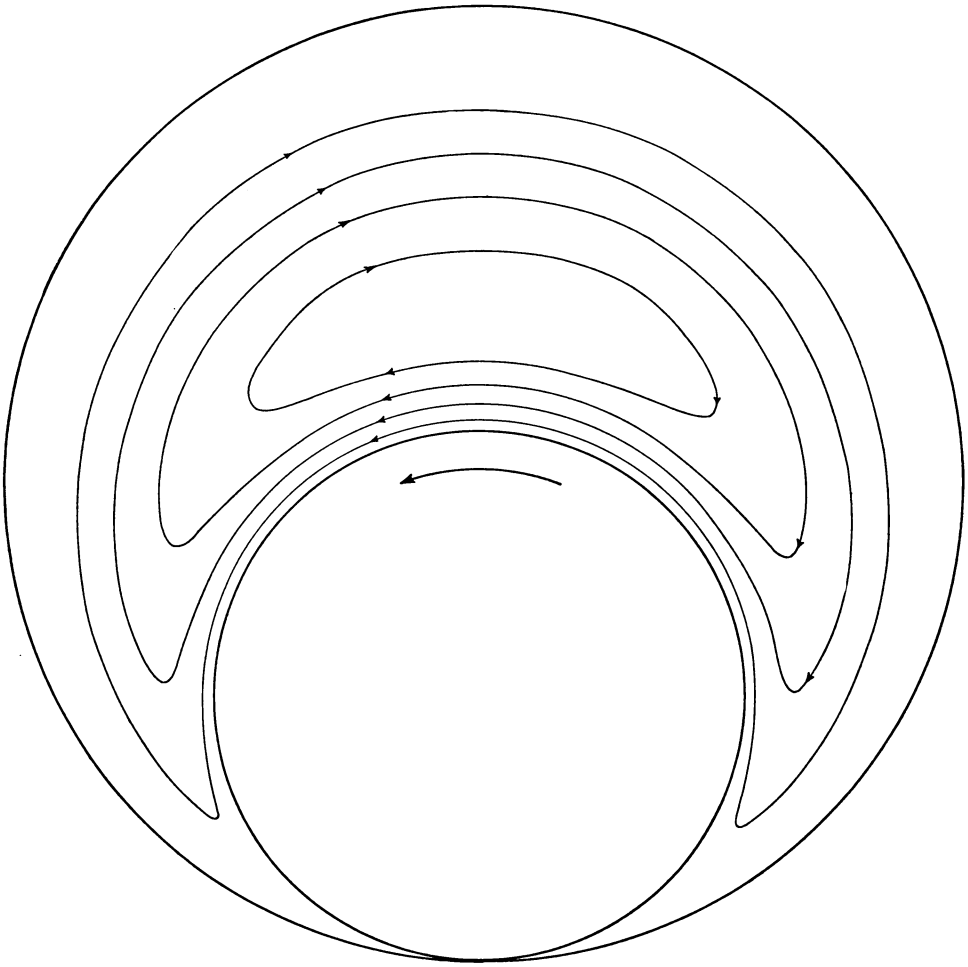

FIG. 9. Streamlines for a journal bearing of diameter ratio 5:9. Full eccentricity (zero clearance).

where r is the conventional radius. The pressure and load are, of course, zero. There remains a shearing stress in the r, ψ direction which is

$$\pi_{r\psi} = -\frac{2\eta a_1^2 a_2^2 (a_1^{-1} v_1 + a_2^{-1} v_2)}{a_2^2 - a_1^2} \frac{1}{r^2}; \tag{49}$$

$2\pi L_r^2$ times this expression is the exerted torque.

(*d*) *Limit of a plane and a cylinder*: d_2, $a_2 \to \infty$; s, d_1, a_1 finite. This interesting limiting case does not alter the nature of the solution obtained, but

greatly simplifies all coefficients. We shall, therefore, keep Eq. (29) and replace (31). Writing

$$d_1 = d, \qquad a_1 = a, \qquad v_1 = v, \qquad v_2 = V,$$

we get

$$A = -\frac{dV}{\log (d+s)/(d-s)} - \frac{1}{2}\frac{dav}{s}, \tag{50a}$$

$$B = \frac{2(d+s)V}{\log (d+s)/(d-s)} + \frac{(d+s)av}{s}, \tag{50b}$$

$$C = \frac{2(d-s)V}{\log (d+s)/(d-s)} + \frac{(d-s)av}{s}, \tag{50c}$$

$$D = -V, \tag{50d}$$

$$E = 0, \tag{50e}$$

$$F = \frac{V}{\log (d+s)/(d-s)}. \tag{50f}$$

The solution decomposes into two parts. The V-part describes a situation where a cylinder falls with velocity V near a vertical wall; the v-part applies when a stationary cylinder rotates with speed v.

If we substitute the expressions (50) into (34a) and (36b) we observe that (a) a cylinder falling in the neighborhood of a vertical wall experiences no torque from it, and (b) a cylinder rotating in the neighborhood of a wall experiences no force from it. In case (a) there is a retarding force equal to

$$W = \frac{8\pi\eta LV}{\log (d+s)/(d-s)}. \tag{51}$$

In case (b) there is a frictional torque equal to

$$T = \frac{4\pi\eta L\, dav}{s}. \tag{52}$$

As an illustration of the formulas obtained, numerical results are shown for a bearing having a diameter ratio 5:9. Figures 7, 8 and 9 show the flow pattern for three different eccentricities: Fig. 7 shows the concentric case (Eq. (48)), Fig. 8 a case of intermediate eccentricity (Eqs. (29) and (31)), and Fig. 9 the case of zero clearance (Eq. (44)). The salient feature of these pictures is the return flow going in a direction contrary to the moving pin. In Fig. 9 the entire flow returns that way, whereas in Fig. 8 only a fraction does. This flow is due, of course, to the pressure difference which forces liquid through the wide section as well as through the narrow clearance. Even in the Reynolds limit of film lubrication this type of flow persists.

Figure 10 shows the pressure distribution for the flow condition of Fig. 8. We can verify on this graph that the pressure generally varies little in direct line from one surface to the other. The Reynolds treatment neglects such variation altogether; this assumption

is thus fairly well justified, even for a bearing of fairly wide clearance. The anti-symmetry of the pressure pattern is more doubtful since it is directly connected with the assumption of incompressibility.

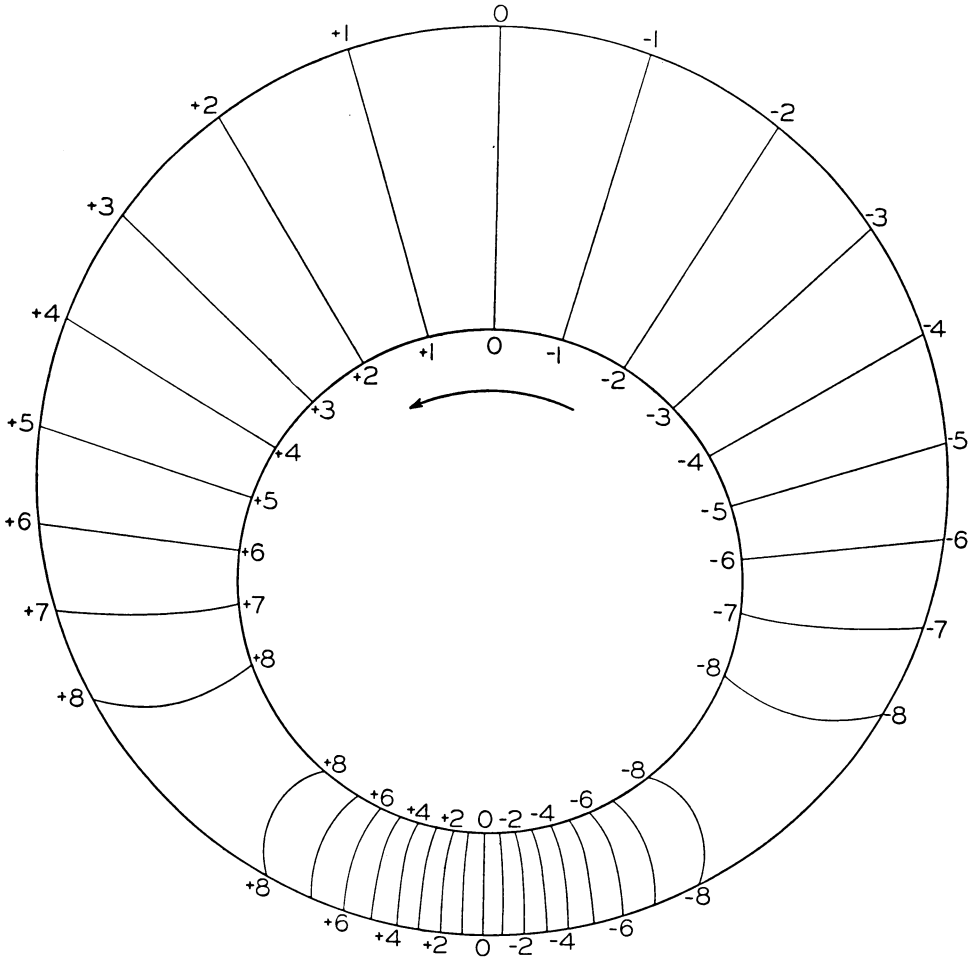

FIG. 10. Lines of constant pressure for the bearing of Fig. 8. Pressures are to an arbitrary scale and contain an additive constant.

Finally, in Figs. 11 and 12, are shown load vs. eccentricity curves and friction vs. load curves for this bearing (Eqs. (35) and (38)). In order to compare them with the traditional Sommerfeld formulas, an intermediate "radius" of 7 is ascribed to the bearing, and Sommerfeld's equations are applied. The differences are not very marked. The graphs do emphasize, however, that there is a difference in the coefficient of friction according to whether it is defined on the inner or outer circle.

4. The spherical bearing. When we pass from rotating cylinders to rotating spheres, we pass essentially from a bearing with line contact to one with point contact. As a consequence, we get "side leakage" of the liquid about the contact point. The presentation to follow gives a partial solution of the mathematical problem. The difficulties

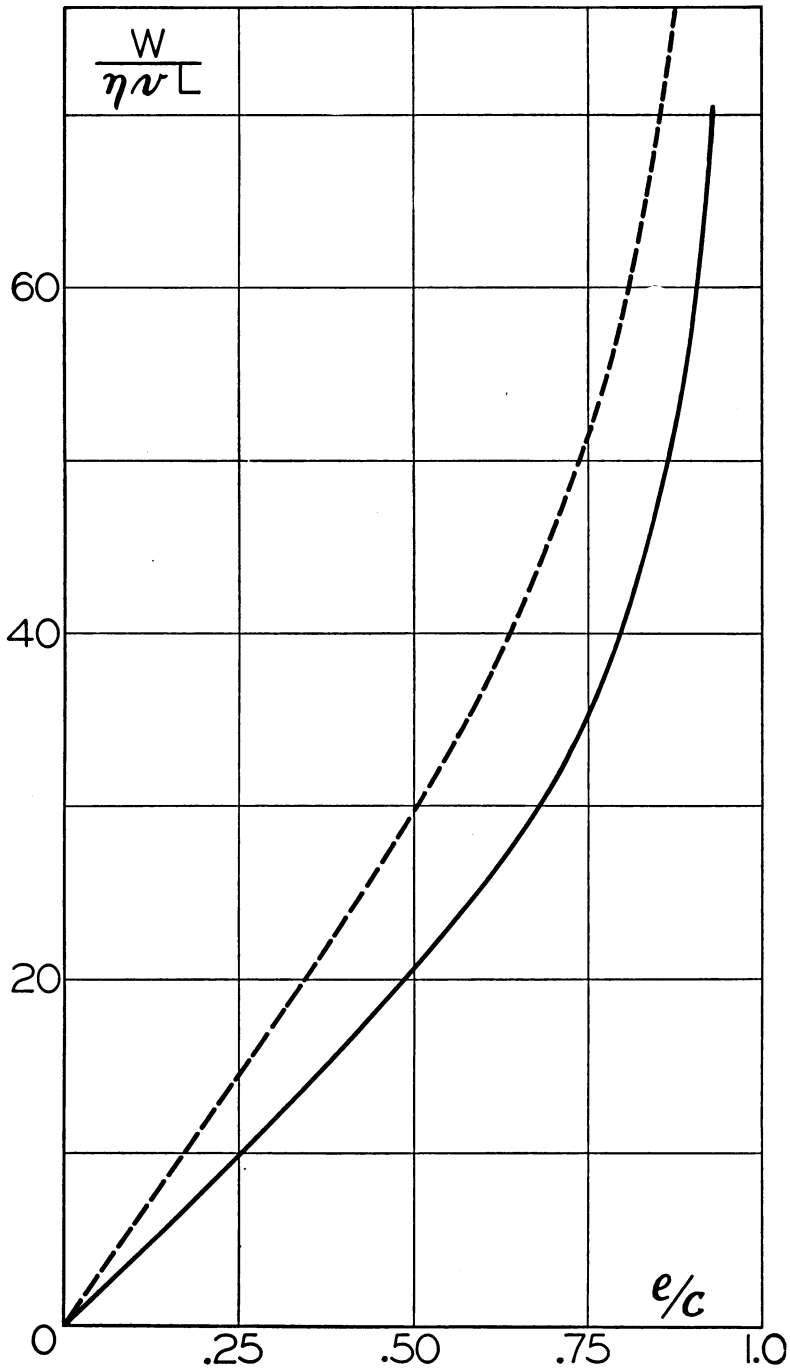

FIG. 11. Load versus eccentricity for a journal bearing of diameter ratio 5:9.
——— Present calculation - - - - Sommerfeld formula
In the figure: W = load, η = viscosity, v = speed of rotation, L = length of journal, e = eccentricity, c = nominal clearance.

encountered are not surprising since the solution for cylinders is based so much on the potential (27) for the same geometry.

In discussing such a bearing there are essentially two possibilities: either the axis of rotation is parallel to the line of centers, or it is perpendicular. Bearings of the former type have been constructed and examined recently by Shaw and Strang.[8] While the bearing apparently works very well, there is at present no complete understanding of its operation. It is easy to show from Stokes' equations (Eqs. (1) and (2)) that if the liquid motion is entirely azimuthal, the pressure in the crescent-shaped cavity is a constant. Actually, there is a slight upward flow in the bearing which is force fed. It may be

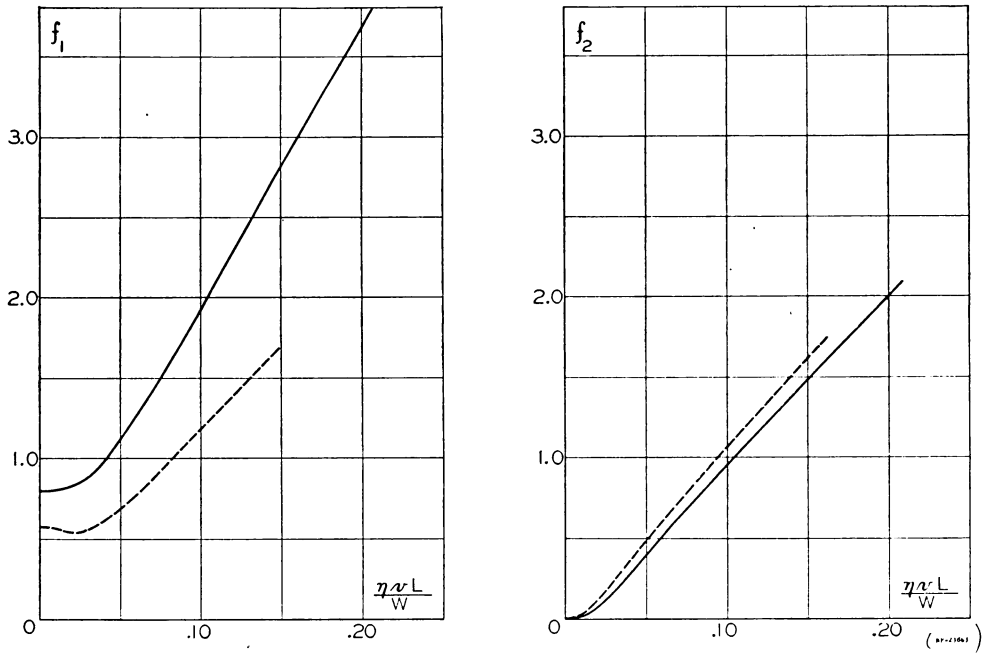

FIG. 12. Coefficient of friction versus load for a journal bearing of diameter ratio 5:9. The left graph defines friction as usual on the inner circle; The right graph defines it on the outer circle.
——— Present calculation - - - - Sommerfeld formula

that here we have simply a tightly sealed-off pocket of liquid which is under the hydrostatic pressure introduced by force feeding the oil. This would make the bearing hydrostatic rather than hydrodynamic, except perhaps for a hydrodynamic effect which prevents contact at the lateral rim.

The normal mode of loading a bearing is lateral. Let the z-axis be the line of centers, and let the x-axis be parallel to the axis of rotation (Fig. 13). The angular velocity will be denoted by ω. The remainder of the nomenclature will be the same as in Fig. 5.

If we introduce a cylindrical coordinate system,

$$\rho^2 = x^2 + y^2, \tag{53}$$

$$\tan \varphi = \frac{y}{x}, \tag{54}$$

[8]M. C. Shaw and C. D. Strang, *The hydrosphere, a new hydrodynamic bearing*, J. Appl. Mech. **15**, 137 (1948).

then the fundamental equations (1) and (2) read,

$$\frac{1}{\eta}\frac{\partial p}{\partial \rho} = \nabla^2 v_\rho - \frac{1}{\rho^2} v_\rho - \frac{2}{\rho^2}\frac{\partial v_\varphi}{\partial \varphi},$$

$$\frac{1}{\eta\rho}\frac{\partial p}{\partial \varphi} = \nabla^2 v_\varphi - \frac{1}{\rho^2} v_\varphi + \frac{2}{\rho^2}\frac{\partial v_\rho}{\partial \varphi},$$

$$\frac{1}{\eta}\frac{\partial p}{\partial z} = \nabla^2 v_z,$$

$$\frac{\partial v_\rho}{\partial \rho} + \frac{1}{\rho} v_\rho + \frac{\partial v_z}{\partial z} + \frac{1}{\rho}\frac{\partial v_\varphi}{\partial \varphi} = 0,$$

and the boundary conditions are,

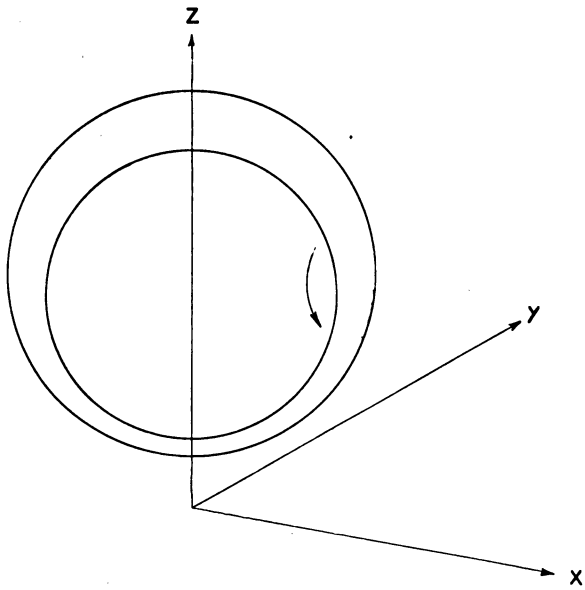

FIG. 13. Coordinate system for the spherical bearing.

on the stationary sphere: $\rho^2 + z^2 - 2d_2 z + s^2 = 0,$

$$v_\rho = 0,$$
$$v_\varphi = 0,$$
$$v_z = 0;$$

on the moving sphere: $\rho^2 + z^2 - 2d_1 z + s^2 = 0,$

$$v_\rho = -\omega(z - d_1)\sin\varphi,$$
$$v_\varphi = \omega(z - d_1)\cos\varphi,$$
$$v_z = \omega\rho\sin\varphi.$$

The form of the equations and boundary conditions is such that the dependence on φ can be eliminated from the equations. We find that

$$v_\rho = f(\rho, z) \sin \varphi, \tag{55a}$$

$$v_\varphi = g(\rho, z) \cos \varphi, \tag{55b}$$

$$v_z = h(\rho, z) \sin \varphi, \tag{55c}$$

$$p = q(\rho, z) \sin \varphi. \tag{55d}$$

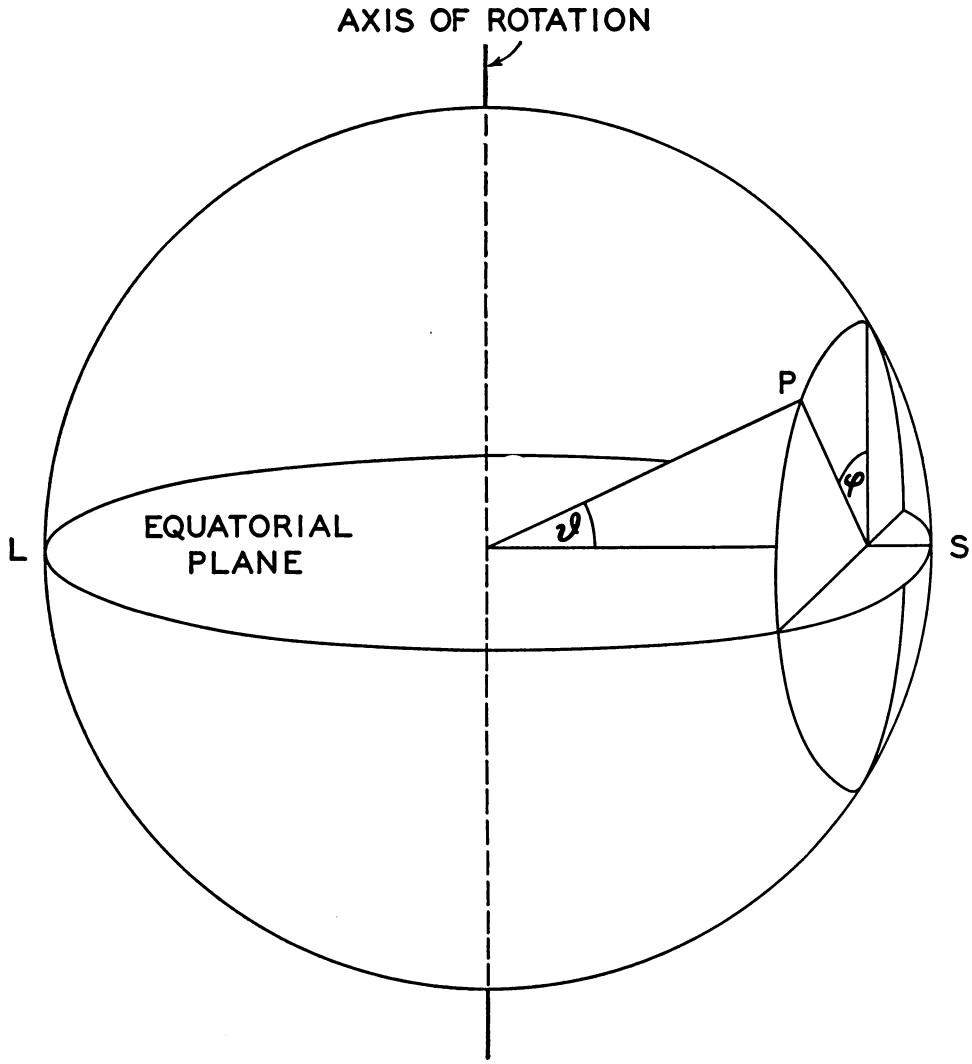

FIG. 14. Polar coordinates for the Sommerfeld type calculation of the spherical bearing. S = point of smallest clearance, L = point of largest clearance.

At this point difficulties are encountered. It is relatively easy to eliminate g and q, but the reduction to one variable does not seem possible. This is the place where the

introduction of the stream function solved the corresponding cylindrical problem. An analogous trick does not seem possible in this case. However, the symmetry of the flow pattern is sufficient to permit the prediction that the resultant force is at right angles to the axis of rotation and the line of centers.

Since the general problem appears insoluble, we shall solve it in the Reynolds limit. This also has not been done up to this time. We place a spherical polar coordinate system into the center of the two spheres, pointing with the polar axis toward the point of least clearance (Fig. 14).

For such a coordinate system the components of the boundary velocity are

$$V_\vartheta = -\omega a \sin \varphi, \tag{56a}$$

$$V_\varphi = -\omega a \cos \vartheta \cos \varphi. \tag{56b}$$

Substituting these expressions into (15), we get

$$\frac{1}{\sin \vartheta} \frac{\partial}{\partial \vartheta} \left\{ h^3 \sin \vartheta \frac{\partial p}{\partial \vartheta} \right\} + \frac{1}{\sin^2 \vartheta} \frac{\partial}{\partial \varphi} \left\{ h^3 \frac{\partial p}{\partial \varphi} \right\} = -6\eta a^2 \omega \sin \varphi \frac{dh}{d\vartheta} \cdot \tag{57}$$

In the coordinate arrangement of Fig. 14 h is only a function of ϑ; in good approximation,

$$h = c - e \cos \vartheta, \tag{58}$$

where c is defined in (39) and e in (24) or Fig. 5. Equation (58) shows, in agreement with (55), that p has the form

$$p(\vartheta, \varphi) = q(\vartheta) \sin \varphi,$$

where $q(\vartheta)$ satisfies an ordinary differential equation. One can verify by direct inspection that this equation has a simple particular integral which is

$$q(\vartheta) = \frac{3\eta a^2 \omega e}{c^2 + e^2/4} \frac{(c - e \cos \vartheta/2) \sin \vartheta}{(c - e \cos \vartheta)^2} \cdot$$

This integral is the only one which is finite at $\vartheta = 0$ and $\vartheta = \pi$. It is, therefore, the correct solution for the closed spherical bearing. The pressure distribution in such a bearing is thus

$$p(\vartheta,\varphi) = \frac{6\eta e a^2 \omega (2c - e \cos \vartheta) \sin \vartheta \sin \varphi}{(4c^2 + e^2)(c - e \cos \vartheta)^2} \cdot \tag{59}$$

There is a remarkable similarity between (59) and (40), particularly if we specialize (59) to give us p along the equatorial plane (see Fig. 14). In this plane $\varphi = \pm\pi/2$, and the azimuth ψ essentially equals ϑ. More precisely, we must substitute

$$\cos \vartheta = \cos \psi,$$

$$\sin \vartheta \sin \varphi = -\sin \psi.$$

Using these substitutions, we find that the dependence of p on the azimuth ψ is exactly the same in the two cases. There is a minor difference in magnitude which shows up best by forming ratios:

$$\frac{p(59)}{p(40)} = \frac{2c^2 + e^2}{4c^2 + e^2} \cdot \tag{60}$$

In view of the inequality

$$0 \leqq e < c,$$

this means that

$$\frac{1}{2} \leq \frac{p(59)}{p(40)} < \frac{3}{5} \cdot \tag{61}$$

It is clear from this analysis that side leakage does not play a very essential role in the theory of lubrication. All the main features are the same in the two cases: the pressure maximum near the point of least clearance, the region of negative pressure on the exit side, the anti-symmetry of the pattern. The factor $\sin \varphi$ gives the continuous transition from the entrance to the exit side, and a factor of the order 1/2 indicates the effect of side leakage on the pressure.

The symmetry of the problem specifies, as pointed out earlier, that the resultant force is at right angles to the line of centers and the axis of rotation. In magnitude, the contribution of π_0, as given by (59), outweighs all others; this may be verified by a study of Sec. 2 or by direct computation.[9] The resultant W is obtained from the formula

$$W = \int_0^{\pi} \sin \vartheta \, d\vartheta \int_0^{2\pi} d\varphi \, p(\vartheta, \varphi) \sin \vartheta \sin \varphi$$

which yields

$$W = \frac{6\pi\eta a^4 \omega}{e^2(4c^2 + e^2)} \left\{ (c^2 + e^2) \log \frac{c + e}{c - e} - 2ce \right\}, \tag{62}$$

where a, c and e are given in (39) and Fig. 4. Now π_0 makes no contribution to the resultant torque. We must pass, therefore, to the next order, which is due to the shearing stress (terms for u which are linear and quadratic in z; see Eq. (5b)). This frictional torque is parallel to the axis of rotation and is obtained on either surface from the formula

$$\pm T = \eta a^3 \int_0^{\pi} \sin \vartheta \, d\vartheta \int_0^{2\pi} d\varphi \left\{ \sin \varphi \frac{\partial v_\vartheta}{\partial r} + \cos \vartheta \cos \varphi \frac{\partial v_\varphi}{\partial r} \right\}.$$

The derivatives in question are obtained from (14), (56) and (59). The result is,

for the inner surface:

$$T_1 = \frac{\pi\eta a^4 \omega}{e^3} \frac{4(c^2 + e^2)}{4c^2 + e^2} \left\{ (c^2 + e^2) \log \frac{c + e}{c - e} - 2ce \right\}; \tag{63a}$$

for the outer surface:

$$T_2 = -\frac{\pi\eta a^4 \omega}{e^3} \frac{2(2c^2 - e^2)}{4c^2 + e^2} \left\{ (c^2 + e^2) \log \frac{c + e}{c - e} - 2ce \right\}. \tag{63b}$$

As above, (Eq. (42)), the torques are not exactly equal and opposite because the fulcrum is in the center of each sphere. If we reduce to the same fulcrum, with the help of (62), the torques check.

[9] Bull. Nat. Res. Council 84, 1932, p. 236. This publication calculates the effect of shear for the Sommerfeld case, but ascribes the wrong direction to it. The more rigorous treatment is also very inappropriate as compared with our Sec. 3.

The coefficients of friction become

$$f_1 = \frac{2(c^2 + e^2)}{3ae}, \tag{64a}$$

$$f_2 = \frac{2c^2 - e^2}{3ae}. \tag{64b}$$

There are some practical difficulties in making the flow pattern of this bearing visible. The general nature of the flow, as given by (14), is the same as for the Sommerfeld bearing; there is a viscous drag flow which varies linearly across the film. This

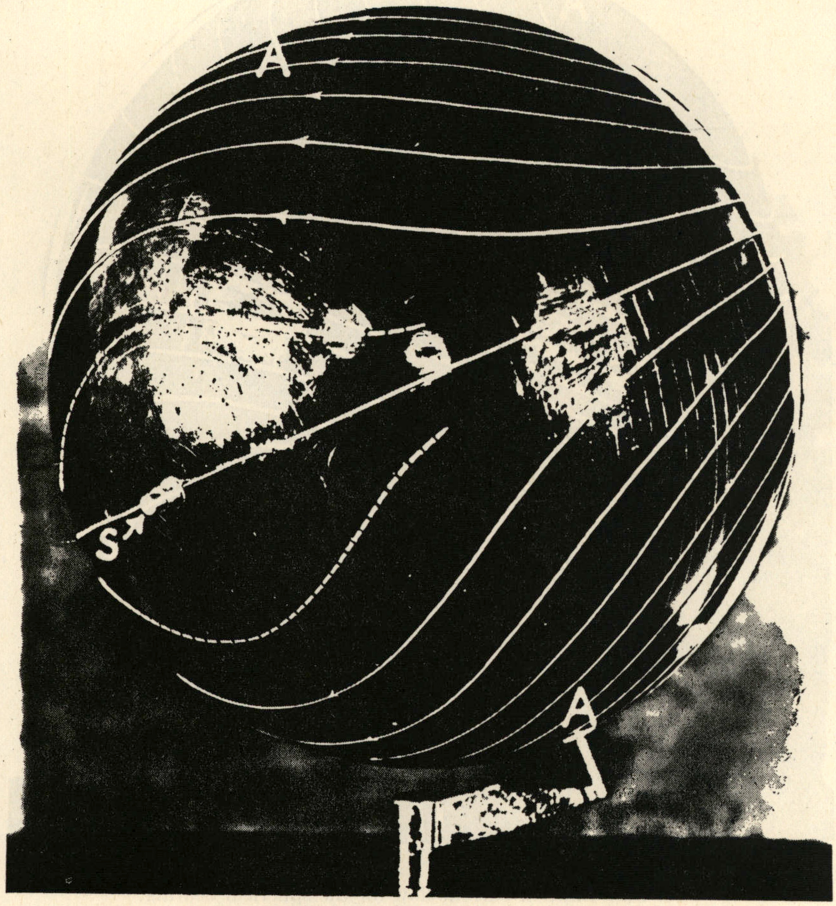

FIG. 15b. Lines of current flow for the spherical bearing.
A = axis of rotation, S = point of smallest clearance.

drag has a tendency to accumulate material on one side; the accumulation is removed by a Poiseuille type flow which varies quadratically across the film. This flow is more complex in the present case than in the Sommerfeld case, for it can go at any angle to the movement of the bearing. The best over-all picture of the flow is gained by showing

the total stream flow Q, that is, the velocity integrated across the film. It results from the formula

$$\mathbf{Q}(\vartheta, \varphi) = \int_0^h \mathbf{V}(\vartheta, \varphi, z)\, dz$$

or from (14a),

$$\mathbf{Q} = \tfrac{1}{2}\mathbf{U}_1 h^2 + \tfrac{1}{3}\mathbf{U}_2 h^3. \tag{65}$$

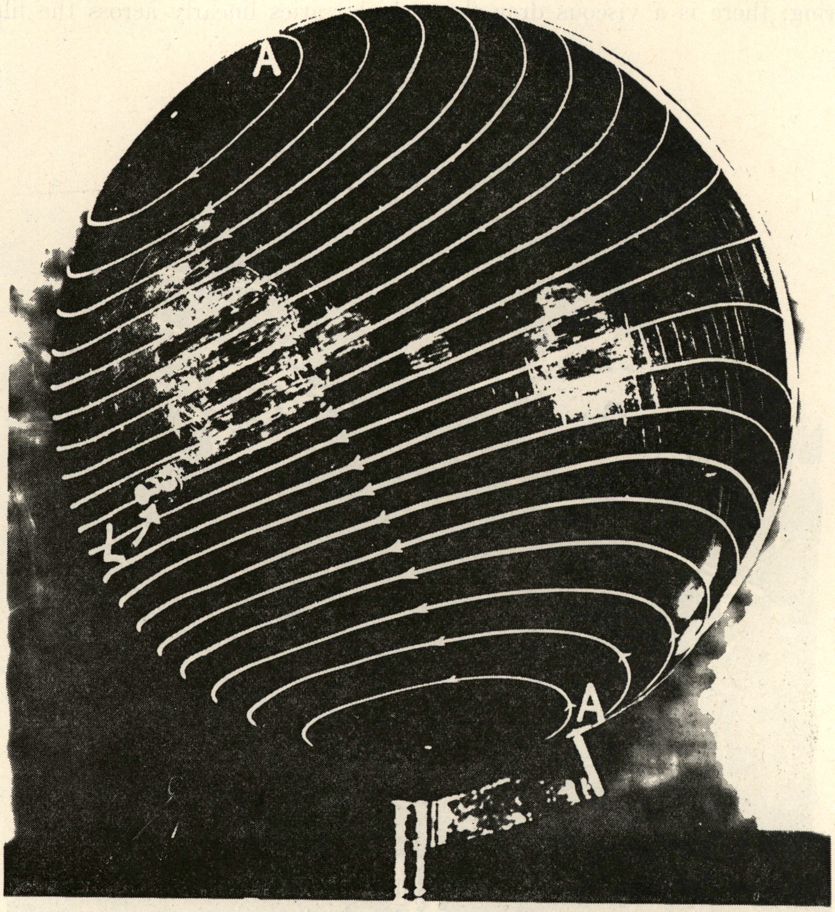

FIG. 15b. Lines of current flow for the spherical bearing.
A = axis of rotation, L = point of largest clearance.

Q is a divergence-free vector in two dimensions and is, therefore, derivable from a stream function Ψ which measures the flow between two points on the spherical film in cm^3/sec. And Ψ is obtained from (60) by either one of the two equations

$$\frac{\partial \Psi}{\partial \vartheta} = -aQ_\varphi \qquad \text{or} \qquad \frac{\partial \Psi}{\partial \varphi} = aQ_\vartheta \sin \vartheta.$$

If we apply Eqs. (14b), (14a), (65) and these last relations successively to (59), we find for Ψ:

$$\Psi = \frac{a^2\omega c}{4c^2 + e^2}(2c^2 - ce\cos\vartheta - e^2)\sin\vartheta\cos\varphi. \tag{66}$$

Two photographs of a plot of this flow pattern on a sphere are shown in Fig. 15. The case picked is the one having the most extreme side leakage when $e = c$. The side leakage around the point of smallest clearance (marked S) is clearly visible. It is also seen that the flow does not take place about the points A which mark the axis of rotation but about a point which is displaced to the side of large clearance. The vortex points, obtained from (66) by setting

$$\Psi(\vartheta, \varphi) = \begin{matrix}\max, \\ \min,\end{matrix}$$

are

$$\cos\vartheta_{\max} = -\frac{1}{2}\frac{e}{c}, \qquad \sin\varphi_{\max} = 0.$$

This indicates a maximum displacement of the vortex by 30°. The total flow between vortices comes out to be

$$\Psi_{\max} - \Psi_{\min} = a^2\omega\frac{(c^2 - e^2/4)^{3/2}}{c^2 + e^2/4}. \tag{68}$$

The flow is thus always smaller than it would be without eccentricity, but there is no change in order of magnitude, in contrast with the cylindrical case.

It should be emphasized that Fig. 15 shows only the integrated flow across the liquid film. The actual velocity varies widely from layer to layer. As an example, we see in Fig. 16 the flow in the layer adjoining the stationary sphere. The flow lines obey the equation

$$\frac{\sin\vartheta\cos\varphi}{|-2c^3 - c^2e\cos\vartheta + 4ce^2 - e^3\cos\vartheta|^{3c^2/(c^2+e^2)}} = \text{const.}, \tag{69a}$$

or for the special case $e \sim c$, $\vartheta \ll \pi/2$,

$$\frac{\vartheta\cos\varphi}{|4(c - e) - c\vartheta^2|^{3/2}} = \text{const.} \tag{69b}$$

The point of minimum clearance is marked M in the figure. There is little resemblance between Fig. 15 and Fig. 16. The essential feature of the latter are the points R which separate two regions of behavior. Along the line RMR the direction of fluid motion coincides with the direction of bearing motion, but outside of R along the same straight line the direction is reversed. We can observe this phenomenon for the cylindrical bearing in Fig. 8, where the corresponding points are also marked R. It is obvious from Fig. 8 that an integrated flow pattern cannot give these essential details.

5. Conclusion. This paper has given formulas of greater rigor and generality than were available heretofore for the cylindrical bearing. As an example, we may mention the new formula for the load carried (Eq. (35)) and the new formulas for the coefficient of

friction (Eqs. (38)). The spherical bearing is brought up to the status which the cylindrical bearing had up to this time by the Eqs. (62) and (64). It is unfortunate, however, that these results are of limited usefulness because of the negative pressure difficulty.

The approach of the research worker to this basic problem has been rather sterile. The negative pressure region has been referred to as "inoperative"[10], and the general

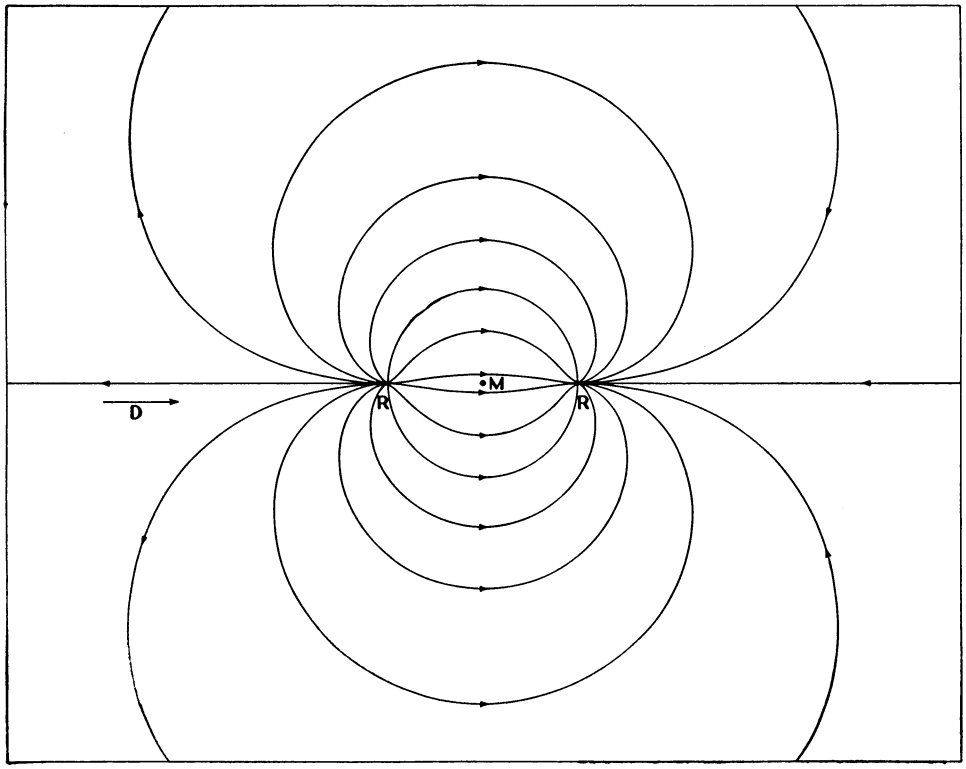

FIG. 16. Flow pattern in the spherical bearing. Flow direction at the stationary surface. Region limited to point of minimum clearance. D = direction of moving bearing surface, M = point of minimum clearance, R = points of flow reversal.

practice has been followed of simply ignoring this region in all integrations. This procedure yields essentially a frictional torque divided by 2 and a load divided by 2 sin α, where α is the angle between load and line of centers. The procedure is intuitively reasonable, but is open to the objection that it is not mechanically sound. Any cut-off line leaves unbalanced stresses acting across it; and if the line of centers is chosen for this purpose, there remains an unbalanced shearing stress which is responsible for the increase in the load obtained. This seems to indicate that we must first understand better the manner in which the liquid cavitates in the "inoperative" region. Then the hydrodynamic equations can be reexamined and corrected accordingly. New values for force and torque will thus result which will be mechanically consistent.

In the absence of such a theory we must adopt a cautious attitude in applying

[10]H. W. Swift, Proc. Inst. Civ. Eng. **233**, 267 (1932).

theoretical formulas. It seems plausible to assume that the *order of magnitude* of the pressure maximum and of its distance from the line of centers would be reasonably safe against modifications because the differential equation is the same on the high pressure side of the bearing. Limiting ourselves to the Sommerfeld limit (although the general case can be handled too by observing that the F term in (27) is generally small compared with the other two and that B and C are very simply related), we can calculate the maximum of (40) and its location. We find that

$$\cos \psi_{\max} = \frac{3ec}{2c^2 + e^2} \tag{70a}$$

or

$$\tan \frac{1}{2} \psi_{\max} = \left[\frac{(2c - e)(c - e)}{(2c + e)(c + e)}\right]^{1/2}. \tag{70b}$$

Formula (70) applies to all loads; but if we are mainly interested in high loads, we can take the combined cases, limit (a) and limit (b) only:

$$c \sim e, \qquad h = c - e \ll c.$$

We then get for the distance D of the pressure maximum from the line of centers,

$$D \sim 2a \tan \frac{\psi}{2} = \left(\frac{2}{3}\frac{h}{c}\right)^{1/2} a.$$

This is written in a more useful form from (39) as

$$D = \left(\frac{2}{3}\frac{h}{1/a_1 - 1/a_2}\right)^{1/2}. \tag{71}$$

It is very satisfactory that only the difference in curvatures enters into (71). This makes D dependent on local conditions only, as postulated. If we substitute (70) into (40) and make the same approximation as above, we get

$$p_{\max} = \left(\frac{27}{32}\right)^{1/2} \frac{\eta v}{(1/a_1 - 1/a_2)^{1/2} h^{3/2}}. \tag{72}$$

This formula also depends on local conditions only, and thus we may expect (71) and (72) to hold under much wider conditions than the derivation given would indicate.

A simple alternative derivation which does not use the film lubrication condition proceeds, for instance, from the plane and cylinder case, limit (d). From (32) and (50) we find that the pressure along the plane has the following form:

$$\frac{1}{\eta} p = -8avd \frac{x}{(x^2 + s^2)^2}.$$

Assuming as before that $d \sim a \gg s$, we get from (26),

$$s^2 = \frac{2h}{1/a_1 - 1/a_2} = 2ha.$$

Maximizing p and substituting s, (71) and (72) follow exactly.

Calculations proceeding from more general assumptions have been prepared by the author. Thus formulas (71) and (72) have so wide a sweep that they can very probably

be applied to convex types of contacts where the curvatures would add, of course. More attention must be paid in this case, however, to other stresses which become more nearly comparable, as the results of limit (d) show.

The difficulties which the theory encounters in the field of lubrication indicate strongly that both theory and experiment should concentrate part of their attention on the negative pressure problem and its possible connection with cavitation. A clear mechanical picture of hydrodynamic lubrication, backed up by quantitative measurements, is probably essential, before modifications of this picture can be discussed with hope of success.

Acknowledgment. In conclusion I wish to thank Mr. Murray L. Deutsch and Mr. Thomas A. Lindland for their valuable help in carrying out the computations.